RESEARCH ARTICLE

Ice-out and freshet fluxes of CO_2 and CH_4 across the air–water interface of the channel network of a great Arctic delta, the Mackenzie

Jolie A.L. Gareis[1] & Lance F.W. Lesack[2]

[1]Department of Geography, Simon Fraser University, Burnaby, BC, Canada
[2]Departments of Geography & Biological Sciences, Simon Fraser University, Burnaby, BC, Canada

Abstract

Carbon dioxide (CO_2) and methane (CH_4) were monitored at five sites spanning the upstream–downstream extent of the Mackenzie Delta channel network during May 2010, capturing the historically under-sampled ice-out period that includes the rising freshet, peak water levels and the early falling freshet (flood recession). Unexpectedly, partial pressures of CO_2 in the Mackenzie River were undersaturated during the rising freshet before water levels peaked, indicating net CO_2 invasion at instantaneous CO_2 flux rates (F-CO_2) ranging from –112 to –258 mg-C m^{-2} d^{-1}. Net CO_2 invasion was also observed around the time of peak water levels at sites in the middle and outer delta. Following peak water levels, the Mackenzie River switched to saturation and net CO_2 evasion (F-CO_2 from 74 to 177 mg-C m^{-2} d^{-1}). Although the Peel River (which flows into the west side of the Mackenzie Delta) was a strong emitter of CO_2 (F-CO_2 from 373 to 871 mg-C m^{-2} d^{-1}), overall, the Mackenzie River and Delta were weak emitters of CO_2 during the 2010 ice-out period. All sites were strong emitters of CH_4 during ice-out, however, with the highest evasive fluxes observed in the outer delta when the extent of flooded delta landscape was greatest. Estimated aerial fluxes from Mackenzie Delta channel surfaces during May 2010 ranged from 2.1 to 4.8 Gg-C as CO_2, and 186 to 433 Mg-C as CH_4. These results provide critical information that can be used to refine gas flux estimates in high-latitude circumpolar river deltas during the relatively under-studied ice-out period.

Keywords

Carbon dioxide; methane; greenhouse gas; Mackenzie River Delta; circumpolar delta; floodplain

Correspondence

Jolie A.L. Gareis, Department of Geography, Simon Fraser University, 8888 University Drive, Burnaby, BC, V5A 1S6, Canada. E-mail: jolieg@sfu.ca

Abbreviations

ANOVA: analysis of variance test
DDI: distilled de-ionized water
DIC: dissolved inorganic carbon
DOM: dissolved organic matter
δ^{13}C-DIC: stable carbon isotope value of the DIC pool
F-CH_4: methane (CH_4) flux
F-CO_2: carbon dioxide (CO_2) flux
F-GAS: instantaneous rate of gas flux across the air–water interface
HDPE: high-density polyethylene
HSD: honestly significant difference test
HYDAT: National Water Data Archive, Canada
pCH_4: partial pressure of CH_4
pCO_2: partial pressure of CO_2
SD: standard deviation

Introduction

Inland aquatic systems are generally net sources that release CO_2 and CH_4 to the atmosphere. Prior studies have quantified the evasion of these globally important carbon-based greenhouse gases from rivers in the tropics (e.g., Richey et al. 2002; Alin et al. 2011; Borges, Darchambeau et al. 2015), temperate zones (e.g., Raymond et al. 1997; Butman & Raymond 2011) and boreal regions (e.g., Wallin et al. 2010; Campeau & del Giorgio 2014). While fluxes from north-flowing rivers have been relatively understudied (Raymond et al. 2013), prior work on some of the world's great circumpolar rivers (Semiletov 1999; Striegl et al. 2012; Bussmann 2013; Denfeld et al. 2013) and smaller stream networks in Alaska (Kling et al. 1992; Crawford et al. 2013) has indicated that all are generally supersaturated in both CO_2 and CH_4 relative to the atmosphere and therefore act as net carbon sources in the northern landscape. However, these studies have mostly taken place during summer flow conditions, while relatively few have measured fluxes during ice-out or the freshet, when both flow rates and water levels reach an annual maximum. Even fewer have investigated flux rates in the productive, lake-rich and seasonally flooded deltas located at the interface between some large circumpolar rivers and the Arctic Ocean. Accurately quantifying CO_2 and CH_4 in these systems is critical because their contribution to total global fluxes may be larger than expected because of gas evasion during ice-out and processes occurring on floodplains during periods of high water.

In northern lakes, ice acts as a seasonal barrier that prevents gas exchange with the atmosphere, resulting in

Citation: *Polar Research* 2020, *39*, 3528, http://dx.doi.org/10.33265/polar.v39.3528

over-winter accumulation of CO_2 and CH_4 to very high concentrations that can rapidly escape to the atmosphere during ice-out. Rates of evasion during ice-out may be the highest observed all year (Phelps et al. 1998; Jammet et al. 2017), with up to 66% of the total CO_2 built up over winter released from Scandinavian lakes in just a few days (Denfeld et al. 2015). In the northern United States, up to 40% of the total annual CH_4 flux from seasonally frozen lakes occurred immediately after ice-out (Michmerhuizen et al. 1996).

Similar to northern lakes, circumpolar rivers and deltas are also ice-covered during each winter. Under-ice decomposition of organic matter from the generally large, forested and organic-rich river basins in which these rivers are situated (Amon et al. 2012), as well as the large concentrations of DIC species derived from groundwater during ice-covered periods (Tank et al. 2012; Gareis & Lesack 2017), together suggest that it is likely that both CO_2 and CH_4 accumulate to high levels under ice in circumpolar rivers and delta channels. It therefore seems probable that evasive fluxes of these gases from circumpolar rivers and delta channel networks would be large and rapid as ice cover is lost at the start of the freshet season, similar to what has been observed in northern lakes. At this time, however, neither the concentrations of these gases under ice nor the magnitude of ice-out fluxes are known for circumpolar lotic systems. This is because the ice-out period is short (generally a few weeks in length) and is characterized by an unstable ice cover, rapidly rising water levels driven by basin snowmelt and moving ice rubble and debris. These conditions make the ice-out period difficult to sample. This critical period has therefore been historically under-sampled in north-flowing river systems, which, in turn, have generally been under-represented in prior estimates of global fluxes of CO_2 (Raymond et al. 2013) and CH_4 (Bastviken et al. 2011; Stanley et al. 2016).

Rates of CO_2 and CH_4 evasion may be even higher than anticipated in circumpolar great rivers that have a delta between their mainstem and the Arctic Ocean. Circumpolar river deltas are large, complex systems containing numerous distributary channels and seasonally flooded lakes. Rising water levels during the early spring freshet cause floodplain lakes to become hydrologically reconnected to delta channels, during which time they are inundated with nutrient- and carbon-rich floodwater. During the subsequent period of flood recession, water that was temporarily stored in floodplain lakes and on the wetted floodplain surface drains back into delta channels. This likely moves large amounts of dissolved gases that were generated under ice in the floodplain lakes back into the channels. Elevated rates of leaching from submerged soils and vegetation, along with aerobic (strongly CO_2-producing) or anaerobic (strongly CH_4-producing, moderately CO_2-producing) decomposition of organic matter, make seasonally flooded systems substantial net sources of dissolved gases to both the atmosphere and downstream regions during inundated conditions (Marani & Alvalá 2007; Abril et al. 2014). Increasing temperatures in high-latitude river deltas at the start of the open-water season may amplify rates of decomposition, releasing labile carbon from thawed permafrost (Vonk et al. 2013; Spencer et al. 2015) and mobilizing a pool of easily-respired substrate from the floodplain that may further increase the production of carbon-based greenhouse gases. When taken together, the above-mentioned considerations indicate that high-latitude river deltas may be hotspots of CO_2 and CH_4 evasion in the Arctic landscape.

The Mackenzie Delta in the western Canadian Arctic is an important representative of the global suite of circumpolar river deltas. To address the general lack of direct measurements of CO_2 and CH_4 in these systems, and the particular lack of these measurements during the high-water flooded periods that occur during ice-out, gas concentrations were measured in Mackenzie Delta channels throughout the 2010 ice-out and freshet. Two sources of river flow to the delta were also sampled: the Mackenzie River, which supplies the vast majority of the delta's inflowing water; and the smaller Peel River (Fig. 1a). Our objectives were to quantify fluxes of carbon-based greenhouse gases from channel surfaces in the Mackenzie Delta during the historically under-sampled ice-out and freshet periods, and to assess downstream changes in gas concentrations and fluxes during the period of peak annual flows and water levels. We expected to find (1) that the delta would remain supersaturated relative to atmospheric gas concentrations throughout the freshet, (2) that partial pressures and fluxes of CO_2 and CH_4 at all sites would be largest when flows and water levels peaked and (3) that fluxes would be greatest at downstream sites because of the addition of dissolved gases generated on the delta floodplain.

Methods

Study area and sampling sites

The Mackenzie Delta forms the interface between the north-flowing Mackenzie River and the Beaufort Sea basin of the Arctic Ocean in the western Canadian Arctic (Fig. 1b). It is the second largest river delta in the circumpolar Arctic and contains wetlands, numerous anastomosing channels and more than 45 000 shallow floodplain lakes that cover almost half of its 13 000 km^2 surface area (Emmerton et al. 2007).

Citation: *Polar Research* 2020, *39*, 3528, http://dx.doi.org/10.33265/polar.v39.3528

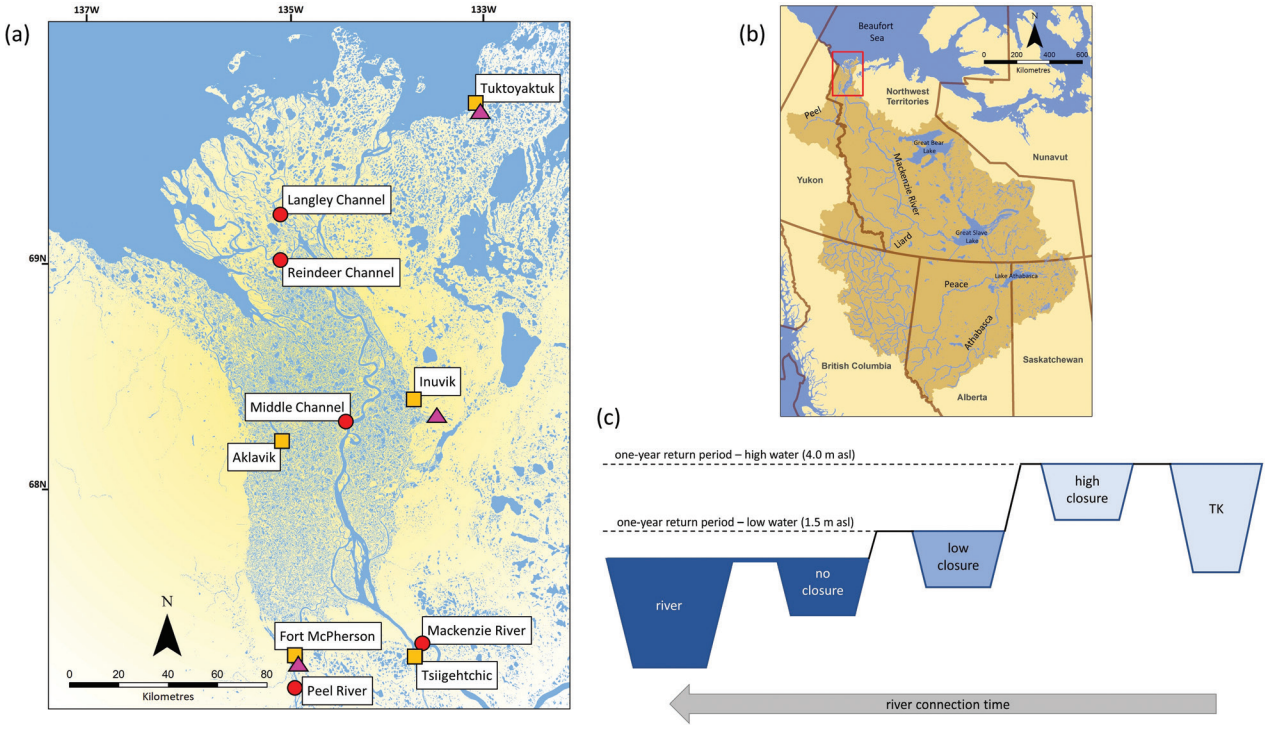

Fig. 1 (a) The Mackenzie Delta. Sampling sites are shown as red dots, towns as yellow squares and Environment and Climate Change Canada meteorological stations as pink triangles. (b) The location of the Mackenzie Delta in the western Canadian Arctic. (c) A conceptual diagram showing the flood frequency gradient of Mackenzie Delta floodplain lakes. Average river-to-lake connection time during the spring freshet increases with decreasing elevation of an individual lake relative to the river channel (Lesack & Marsh 2010). Thermokarst lakes (here labelled "TK") are a subset of the high closure lake class formed by thawing ice-rich permafrost that are deeper on average than non-thermokarst lakes.

The Mackenzie River and Delta are ice-covered for seven to eight months each winter, followed by ice-out and the spring freshet, when the system returns to open-water conditions. The spring freshet is initiated when snow- and ice-melt in the 1.8×10^6 km^2 Mackenzie Basin generate an increase in the rate of discharge of more than 3% per day in the Mackenzie River upstream of its delta (Lesack et al. 2013). Peak freshet discharge averages 27 600 m^3 s^{-1} in the Mackenzie River (1973–2015 average at the Water Survey of Canada hydrometric gauging station 10LC014 [HYDAT 2019]), with discharge during the freshet being greater than during any other time of the year. As the freshet moves downstream (north) into the Mackenzie Delta, it encounters the still-frozen ice cover in delta distributary channels. The mechanical force of the freshet can fracture the ice, which accumulates in delta channels and forms dams that are referred to as "ice jams." When ice jams restrict the downstream flow of the freshet, already-high water levels in delta channels are further raised (Beltaos 2012; Lesack et al. 2013), leading to overbank flooding and inundation of the delta landscape. On an average, just less than half (25.8 km^3) of the total freshet discharge volume (55.4 km^3) moves off-channel and onto the delta floodplain for some amount of time each year (Emmerton et al. 2007). Lakes on the Mackenzie Delta floodplain become hydrologically reconnected to delta channels during the freshet, with lakes sitting at lower elevations relative to the nearest distributary channel remaining connected for longer periods than those perched at higher elevations (Fig. 1c).

Five sampling sites were chosen to capture the greatest proportion of flow possible in three delta transects (Fig. 1a). The inflow river transect included two sampling sites in the Mackenzie and Peel rivers upstream of the delta. The Mackenzie River has a Subarctic nival regime and contributes ca. 95% of the total water flow received by the delta in all seasons (Morley 2012), while the Peel River has a catchment area of 73 600 km^2 and drains a mountainous basin to the west side of the Mackenzie Delta. The Peel contributes a greater percentage of the total flow into the delta during the summer (7.0%) than during the ice-covered winter season (3.1%) (Morley 2012). The middle delta transect was sampled at a single site on the Middle Channel, which carries between 79 and 89% of the total flow in this transect (Morley 2012). The outer delta transect was sampled at two sites (Langley and

Reindeer channels) that were upstream of any tidal influence from the Beaufort Sea, which was confirmed by taking a measurement of conductivity prior to sampling. Detailed analysis of the hydrology of the Mackenzie Delta has suggested that these two channels collectively export approximately 50% of the total delta outflow (Morley 2012). All sites were sampled throughout May 2010, when ice-out typically occurs in the network of delta channels, capturing the rising freshet, peak discharge (19 May 2010) and the immediate post-flood high water period (Fig. 2). This ice-out period in the channel network occurs at the same time as the ice-out period for lakes on the Mackenzie Delta floodplain. Sampling in the Mackenzie River continued throughout the falling freshet until early July 2010.

Hydrometric data (discharge or water level) were retrieved from HYDAT (Fig. 2). Discharge data were available for the Mackenzie River, Peel River and Middle Channel site in the middle delta transect. In outer delta channels, complicated interactions between water level and discharge occur during periods of backwater conditions, which are caused by ice jams during the freshet and storm surges during periods of open water (Beltaos 2012; Blackburn et al. 2015). These conditions prevent the determination of accurate discharge data and, as a result, only water level data were available from HYDAT for outer delta sites.

Field sampling

Water samples for the determination of DIC parameters were collected in acid-washed (10% HCl), DDI-rinsed (10 times) and sample rinsed (three times) HDPE bottles. Water samples for the determination of gas concentrations were collected in evacuated 160 ml glass serum bottles that were prepared following standard procedures (e.g., Hamilton et al. 1994; Cunada 2016). Serum bottles were soaked for 12 hours (10% HCl), DDI-rinsed (10 times) and allowed to air dry. A total of 8.9 g of KCl was added to each serum bottle as a preservative (Hesslein et al. 1991) to prevent bacterial growth while leaving the pH of the water sample unaltered. Serum bottles were sealed with rubber septa and completely voided of air using a vacuum pump. A syringe of ambient air was then used to inject a 10 ml headspace into each serum bottle. Triplicate samples of ambient air were taken so that the initial concentrations of CO_2 and CH_4 in the headspace could be measured and subsequently deducted from sample concentrations. Serum bottles prepared in this fashion have been stored for up to two months with no loss of vacuum (Hamilton et al. 1994), although all bottles used herein were prepared less than two weeks before sampling.

The method used to collect samples at channel sites was determined by the prevailing ice conditions. If the channel ice cover was still intact and sturdy enough to support the weight of a helicopter, samples were collected through an augered hole in the ice surface. A weighted, slow-filling sampler was continuously raised and lowered through the water column under the ice to collect an integrated water sample that was emptied into a 10 L bucket, from which all DIC and gas samples were taken. After the channel ice had broken up to the point where it could no longer safely support the weight of a helicopter, the helicopter instead landed on pontoons on the channel surface in a stretch of open water. A 10 L bucket

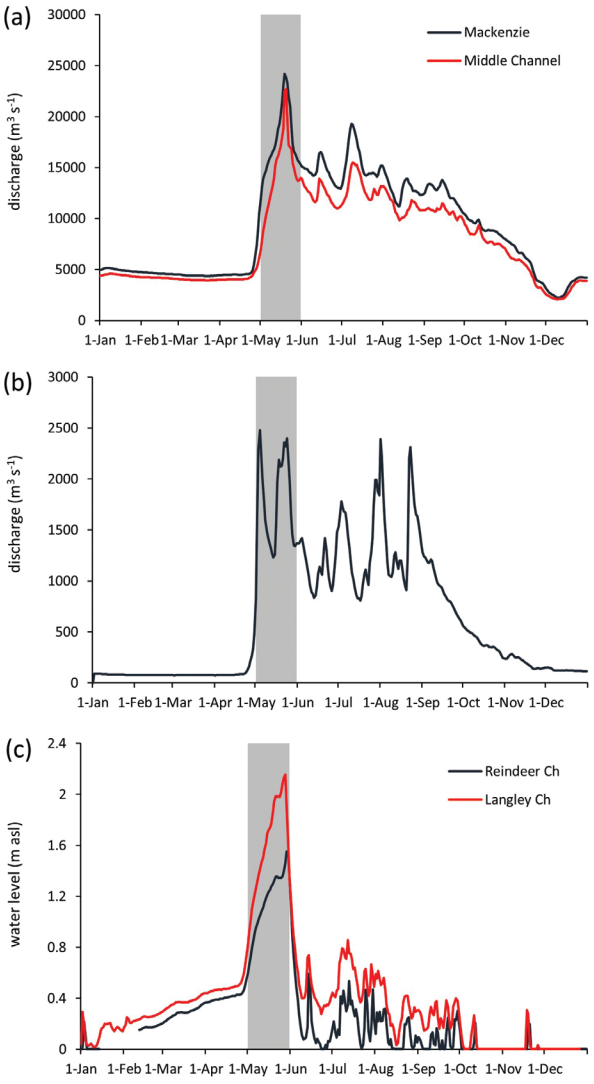

Fig. 2 Hydrological data for the Mackenzie Delta system during the 2010 calendar year. Discharge (Q; $m^3 s^{-1}$) for the (a) Mackenzie River (inflow transect) and Middle Channel (middle delta transect) and (b) Peel River (inflow transect), and (c) water level (m a.s.l.) in the two outer delta channels, the Reindeer and Langley Channels. In all graphs, the shaded area delineates the period over which delta-wide gas fluxes (presented in Table 2) were estimated (1–31 May 2010).

Citation: *Polar Research* 2020, *39*, 3528, http://dx.doi.org/10.33265/polar.v39.3528

was used to collect surface water, from which gas samples were taken, while DIC samples were taken directly from the channel by submerging a 1 L HDPE bottle well below the water surface. During the falling freshet, the Mackenzie River was sampled by collecting surface water in a 20 L bucket lowered over the side of a commuter ferry, from which all DIC and gas samples were taken.

In each case, three gas samples were taken from a single water sample by submerging serum bottles below the water surface in the bucket and piercing each septum with a 16G needle. When water flow into the bottle ceased, the needle was removed and the bottle left submerged for one min to ensure that the septum had fully resealed. The serum bottles were gently swirled to dissolve all KCl and stored in dark, cool (4 °C) conditions during transport (less than eight hours) to the Inuvik Research Centre in Inuvik, Northwest Territories. Our sampling method using a large bucket therefore yielded three pseudoreplicates from a single water sample, which allowed us to assess the replicability of our sample analysis. While using a large bucket to collect water samples allowed us to repeatedly sample the Mackenzie River and Delta channels under challenging field conditions during the freshet, the turbulence it created may have caused some gas to evade prior to sub-sampling. This is particularly likely to have happened when an integrated sample was emptied from the sampler into the bucket. As a result, the gas concentrations and fluxes presented herein are conservative low-end estimates of real-world conditions.

Laboratory analyses

DIC. Water samples were filtered through Millipore membrane filters (filter code GPWP, 0.2 µm pore size) and stored in acid-, DDI- and sample-rinsed borosilicate vials. Concentrations of DIC and δ^{13}C-DIC were measured using a modified OI 1010 total organic carbon wet chemical oxidation analyser coupled to a Thermo Delta Plus XP isotope ratio mass spectrometer following the methods of Osburn & St.-Jean (2007). Samples were injected into the wet chemical oxidation analyser, acidified and sparged to drive all inorganic carbon out of solution as CO_2 gas, which was quantified as DIC using a nondispersive infrared detector. CO_2 gas was then carried into the mass spectrometer in a stream of ultra-high purity He for measurement of δ^{13}C. Stable isotope values for DIC are reported in per mille units (‰):

$$\delta^{13}\text{C-DIC} = [(R_{sample}/R_{std})-1] \times 1000, \quad (1)$$

where R_{sample} is the ratio of $^{13}C/^{12}C$ in the sample and R_{std} is the ratio of $^{13}C/^{12}C$ in the CO_2 reference gas. Values of δ^{13}C-DIC were normalized to the Vienna Pee Dee Belemnite international scale using solutions of oxalic acid (–18.3‰) and L-glutamic acid (–26.2‰).

Dissolved gases. Samples were warmed to room temperature and shaken for 20 min using a wrist-action shaker to equilibrate the gas and liquid phases. A gas-tight syringe was used to extract headspace gas for analysis on a Varian 3800 gas chromatograph that used a thermal conductivity detector to measure CO_2 concentrations, and a flame-ionizing detector to measure CH_4 concentrations. For each sample run, a four-point calibration curve was constructed using gas standards (48, 347, 912 and 5823 ppm for CO_2; 54, 359, 928 and 5946 ppm for CH_4).

Headspace gas concentrations were adjusted to account for the ambient CO_2 and CH_4 present in the original headspace, and corrected to give in situ concentrations (C_W; µmol L^{-1}) and partial pressures (pCO_2, pCH_4; µatm) using gas-specific constants corrected for salinity (resulting from the addition of KCl preservative) and water temperature (EPA 2004; Sander 2014). Henry's Law Constant was used for CO_2, following the methods of Weiss (1974), while the Bunsen solubility coefficient was used for CH_4, following the methods of Yamamoto et al. (1976).

Concentrations of each gas in equilibrium with the atmosphere (C_A; µatm) were also determined using atmospheric levels of CO_2 and CH_4. These were assumed to be 395.5 and 1.9 µatm, respectively, which were derived from the average atmospheric concentrations in dry air during the sampling period at the nearest Global Greenhouse Gas Reference Network site in Barrow, Alaska (71.323°N, 156.611°W; NOAA ESRL Global Monitoring Division 2016; Dlugokencky et al. 2019).

Analytical constraints in early May, and the loss of one sample during shipping, prevented direct measurement of gas concentrations in a total of six samples. Although CH_4 concentrations could not be reconstructed, missing CO_2 concentrations were calculated using total alkalinity, DIC concentrations and pH. Alkalinity was determined using Gran's plot analysis of acid titration curves (Gran 1952). The resulting data points (CO_2 concentrations and fluxes from all sites on 5 May and from the Middle Channel on 24 May) should be considered conservative estimates of actual gas concentrations because gas may have evaded from the water sample during storage.

Calculations of F-GAS

Values of *F*-GAS (µmol m^{-2} h^{-1}) were calculated as:

$$F\text{-GAS} = 10\ k_{GAS}\ (C_W - C_A), \quad (2)$$

where k_{GAS} is a gas-specific transfer velocity (cm h^{-1}), C_W is the gas concentration in water (µmol L^{-1}), C_A is the gas

concentration in equilibrium with the overlying atmosphere (μmol L^{-1}) and 10 is a unit conversion factor. Negative values of *F*-GAS indicate a gas flux from the atmosphere into the water body (invasion), while positive values indicate a gas flux out of the water body to the atmosphere (evasion). Gas fluxes expressed as moles of gas per unit area per hour were then converted to flux rates expressed as the mass of carbon per unit area per day (mg-C m^{-2} d^{-1}).

We were not able to directly measure k_{GAS} during our study. The floating chamber method (Frankignoulle 1988) is frequently used in gas flux studies in aquatic systems to determine gas-specific transfer velocities (k_{GAS}) that are specific to the conditions of the study system. This method requires direct measurement of changes in gas concentrations over time in a closed headspace directly above the air–water interface. During our study, however, neither the conditions at the time of sampling (moving ice in delta channels), nor our method of accessing sampling sites (either by helicopter or commuter ferry), permitted repeated measurements of a closed headspace over time. We therefore used a range of CO_2-specific gas transfer velocities (k_{CO2}) for large rivers and estuaries that were published by Raymond & Cole (2001). This range of k_{CO2} values (3–7 cm h^{-1}) is likely lower than real-world values in the Mackenzie Delta channel network (see the Discussion), so we propose that the flux values presented herein are conservative estimates. We have included further information on system conditions affecting gas transfer velocities, and other methods of estimating k_{GAS} for comparative purposes, in the Supplementary material.

Gas transfer velocities for CH_4 (k_{CH4}) were found using the high and low limits for k_{CO2} (3 and 7 cm h^{-1}) and the following equations:

$$k_{600} = k_{CO2} \times (600/Sc\text{-}CO_2)^{-0.5} \quad (3)$$

$$k_{CH4} = k_{600} \times (600/Sc\text{-}CH_4)^{0.5}, \quad (4)$$

where Sc-CO_2 and Sc-CH_4 are the temperature-dependent Schmidt numbers calculated according to the methods of MacIntyre et al. (1995) and Wanninkhof (1992), respectively.

F-GAS was calculated using daily gas concentration data from each site, and both the high and low limit for the applicable gas transfer velocity, yielding two flux estimates (high and low) for each gas. For CO_2, the flux equation was further modified to account for potential chemical enhancement of flux rates due to the rapid dissociation of H_2CO_3 to (HCO_3^- + H^+) in the water column using the dimensionless enhancement factor α:

$$F\text{-}CO_2 = 10\, k_{CO2}\, \alpha\, (C_W - C_A) \quad (5)$$

Chemical enhancement is greater at high pH, low wind speeds and low values of k_{600} (Wanninkhof & Knox 1996). The flux of CO_2 was calculated with no enhancement when $C_W > C_A$, but with enhancement when $C_W < C_A$. Including chemical enhancement in CO_2 flux calculations generally increased the rate of invasion by less than 2%.

Calculations of ice-out fluxes across the air–water interface of the channel network

The total flux of both CO_2 and CH_4 from the Mackenzie Delta channel network during ice-out was estimated for the month of May 2010. Each delta transect (inflow rivers, middle delta and outer delta) was first considered individually. For the inflow transect, *F*-GAS values from the Mackenzie and Peel on each sampling day were weighted using river discharge. The resulting flow-weighted daily flux rates were then averaged for the rising freshet (1–19 May) and early flood recession periods (20–31 May), multiplied by the number of days in each period (19 and 12, respectively), and multiplied by the total channel surface area in the inflow transect (as determined by Emmerton et al. [2007]). The fluxes for the rising freshet and early flood recession periods were then summed to give a total inflow transect flux for each gas during May 2010. The smaller number of samples that were taken in the middle and outer delta transects did not allow the rising freshet and early flood recession periods to be analysed separately. Instead, for the middle and outer delta transects, instantaneous fluxes were averaged over all sampling days in May, multiplied by the number of days in the month (31), and then multiplied by the total channel surface area in each transect (as determined by Emmerton et al. [2007]). As a final step, fluxes from each transect were summed to give a total delta-wide flux for each gas during the month of May 2010. Using similar methods, fluxes were also estimated across the entire open-water season of 2010, which started on 25 April and continued to 25 October, the last ice-free day in the fall. To evaluate the effect of including data from the rising freshet period, all fluxes were recalculated with rising freshet data from the inflow transect excluded.

Data analysis

Significant differences in the average concentration of excess gas (C_W–C_A) were examined among all sites using a one-way ANOVA on base-10 log transformed data, followed by a Tukey HSD post-hoc test to account for the error accumulation associated with multiple tests. Differences in the average *F*-GAS generated by our high

Citation: *Polar Research* 2020, *39*, 3528, http://dx.doi.org/10.33265/polar.v39.3528

(7 cm h^{-1}) versus our low (3 cm h^{-1}) limits on the gas transfer velocity (k_{CO2}) were examined among sites using paired *t*-tests. We acknowledge that our approach, which grouped all data at a sampling site across all sampling dates, assumed that there was no temporal autocorrelation in our data sets. In all cases, data from the Mackenzie River and the Middle Channel site in the middle delta transect were grouped together, both because of the small number of samples at the Middle Channel site and because the influence of the Mackenzie River dominates any other influence (e.g., Peel River, outflow from the delta floodplain) at the Middle Channel site (Morley 2012). All statistical analyses were performed using JMP statistical software (version 13.1.0).

Results

Patterns in gas concentrations during the 2010 freshet

Values of pCO_2 in the Mackenzie River (average ± SD 232 ± 80 µatm) were well below atmospheric equilibrium (395.5 µatm) during the rising freshet (Fig. 3a, Table 1a). As the freshet progressed, pCO_2 increased above atmospheric equilibrium shortly after peak water levels were reached and remained high throughout the falling freshet (average ± SD 581 ± 244 µatm). When plotted against discharge, pCO_2 showed an anti-clockwise hysteresis with higher partial pressures on the descending limb of the hydrograph compared to the ascending limb (Fig. 4a),

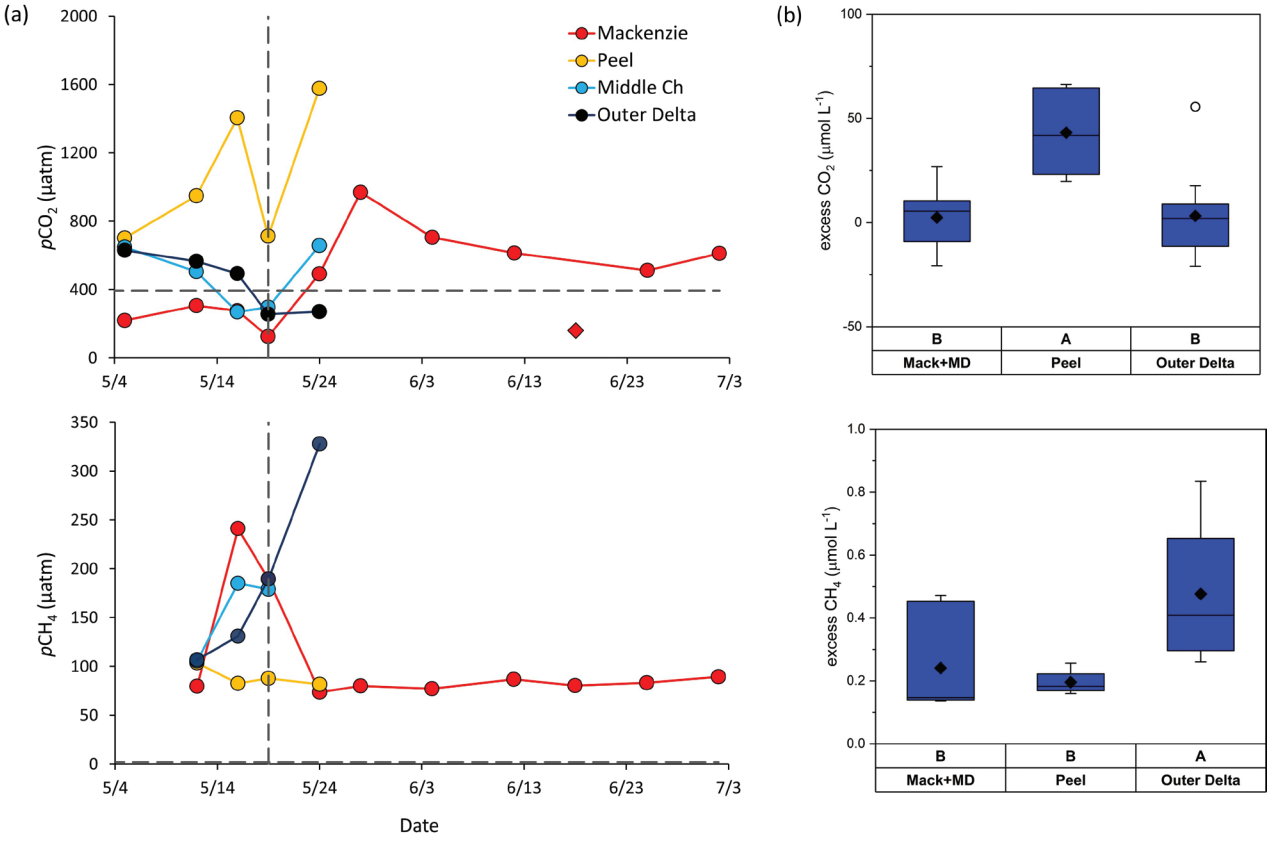

Fig. 3 Gas concentration data for the Mackenzie River and Delta channels during the 2010 freshet. (a) Partial pressures (µatm) of CO_2 (top) and CH_4 (bottom). In both graphs, the dashed vertical line indicates the day of peak discharge in the Mackenzie River (19 May 2010), while the dashed horizontal lines indicate the atmospheric concentrations of each gas (CO_2 = 395.5 µatm, CH_4 = 1.9 µatm). The red diamond in the pCO_2 graph denotes an anomalous data point (18 June 2010) that was excluded from all analyses. Note that there are no CH_4 data shown for the Middle Channel on 24 May 2010 because the sample was lost in transit. (b) The excess gas (concentration in water relative to the concentration in air) for CO_2 (top) and CH_4 (bottom). Note that the Mackenzie River and Middle Channel sites were grouped together (Mack+MD). Boxplots show medians and quartiles (boxes), averages (filled diamonds), 90% confidence intervals (whiskers) and ranges (hollow dots). In each graph, those sites accompanied by the same letter (shown below each boxplot) had mean values that were not significantly different from one another ($p > 0.05$) according to a one-way ANOVA on base-10 log transformed data, followed by a Tukey HSD post-hoc test.

Table 1 Partial pressures (µatm) and *F*-GAS (mg-C m^{-2} d^{-1}) of CO_2 and CH_4 from (a) the 2010 ice-out and freshet in the Mackenzie River and Delta, and (b) prior studies of large river and floodplain systems. For (a) partial pressures are presented as averages (SD), and flux rates are presented as the low and high estimates of the average found using the limits on the gas transfer velocity proposed for large rivers and estuaries by Raymond & Cole (2001). For (b) partial pressures and fluxes may be presented as averages (SD), ranges (minimum–maximum) or in another fashion, depending on how results were reported in the source material.

Reference	System	pCO_2 (µatm)	*F*-CO_2 (mg-C m^{-2} d^{-1})	pCH_4 (µatm)	*F*-CH_4 (mg-C m^{-2} d^{-1})
(a) This study	Mackenzie River (rising freshet)	232 (80)	[–258 – (–112)]	170 (82)	(3.6 – 8.5)
	Mackenzie River (falling freshet)	581 (244)	(74 – 177)	81 (5)	(1.2 – 2.8)
	Peel River	1069 (402)	(373 – 871)	89 (10)	(1.7 – 3.9)
	Middle Delta (Mackenzie Delta)	475 (186)	(51 – 119)	157 (44)	(3.4 – 7.9)
	Outer Delta (Mackenzie Delta)	441 (289)	(27 – 65)	189 (92)	(4.1 – 9.5)
(b) Prior studies					
	Circumpolar river systems				
Telang 1985	Mackenzie River	4663 (3893)			
Vallières et al. 2008	Mackenzie Delta channels	694			
Tank et al. 2009	Mackenzie Delta lakes		(–600 – 1600)		
Cunada 2016	Mackenzie Delta lakes (ice-out)	> 4000		50 – 8000	72
Bussmann et al. 2017	Lena River Delta				(0.05 – 1.96)
Striegl et al. 2012	Yukon River		2055		14.4
Lauerwald et al. 2015	Yukon River	(582 – 705)	(380 – 696)		
Kling et al. 1992	Kuparuk River	812 (811)	143 (83)	236	4
Semiletov 1999	Kolyma River	(716 – 1779)			
Denfeld et al. 2013	Kolyma River	613 (315)	500 (700)		
Bastviken et al. 2011	Global rivers > 66° N				7
Lauerwald et al. 2015	Large rivers > 50° N	(888 – 1086)	(251 – 364)		
	Other large river systems at lower latitudes				
Alt 1993	St. Lawrence River	2322 (214)			
Cole & Caraco 2001	Hudson River	1062 (417)	(192 – 444)		
Alt 1993	Mississippi River	4593 (183)			
Pulliam 1993	Ogeechee River floodplain		2518		271
Butman & Raymond 2011	Temperate rivers, 25 – 50° N		6500		
Gan et al. 1983	Yangtze River	1222 (264)			
Borges, Darchambeau et al. 2015	Sub-Saharan rivers	6415	(2931 – 3950)	35	(86 – 118)
Alin et al. 2011	Mekong River	(703 – 1597)	1384 (1182)		
Borges et al. 2018	Mekong Delta	(479 – 2664)	397 (187)	< 3.5	1.1 (0.6)
Alin et al. 2011; Borges, Abril et al. 2015	Amazon River	(1600 – 6037)	(530 – 3008)		
Richey et al. 2002	Amazon River and floodplain		2274 (658)		
Dalmagro et al. 2018	Pantanal	(5973 – 14 292)	320	(2956 – 51 675)	20
Stanley et al. 2016	Worldwide			2165	(< 0.01 – 486)

indicating that the river only acted as a source of CO_2 to the atmosphere during the later stages of the freshet. Sites in the middle and outer delta declined from above- to below-atmospheric equilibrium during the rising freshet, while in contrast, pCO_2 for the Peel River remained well above equilibrium (average ± SD 1069 ± 402 µatm) throughout the sampling period (Fig. 3a, Table 1a).

Values of pCH_4 in the Mackenzie River remained well above atmospheric equilibrium throughout the freshet, reaching a peak of 241 µatm shortly before peak flood (Fig. 3a, Table 1a). Partial pressures then declined and were relatively constant (74–89 µatm) for the remainder of the falling freshet, indicating a strong net evasion from the Mackenzie during the high-water period. Values of pCH_4 displayed clockwise hysteresis, with higher concentrations on the ascending limb of the hydrograph as opposed to the descending limb, indicating that the river was a greater source of CH_4 to the atmosphere during the early freshet (Fig. 4b). At downstream delta sites pCH_4 values increased rapidly around the time of peak flood, while remaining relatively constant in the Peel River throughout the freshet (average ± SD 89 ± 10 µatm; Fig. 3a, Table 1a).

Citation: *Polar Research* 2020, *39*, 3528, http://dx.doi.org/10.33265/polar.v39.3528

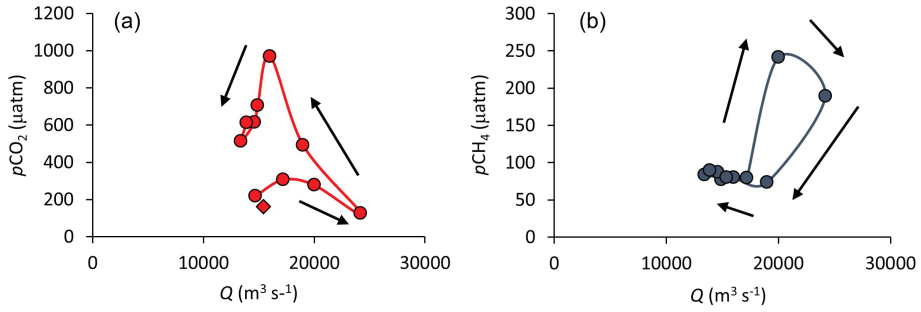

Fig. 4 Partial pressures (µatm) of (a) CO_2 and (b) CH_4 versus discharge (Q), as measured in 2010 at the Mackenzie River sampling site immediately upstream of the Mackenzie Delta. Both gases show hysteresis, but in opposite directions (anticlockwise for CO_2, clockwise for CH_4). The red diamond in the CO_2 graph is an anomalous data point (18 June 2010) that was excluded from the trend analysis.

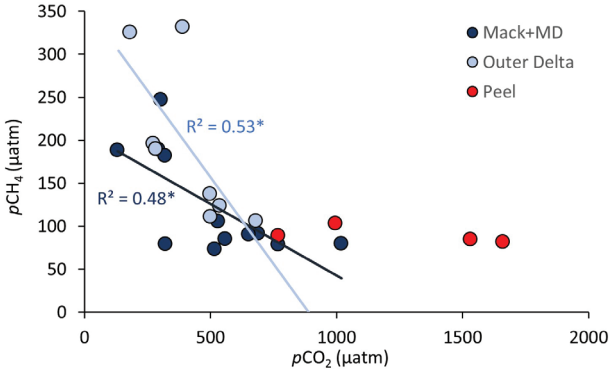

Fig. 5 Partial pressures of CO_2 (pCO_2, µatm) versus CH_4 (pCH_4, µatm) measured at Mackenzie Delta channel sampling sites during the 2010 freshet. Note that the Mackenzie River and Middle Channel sites were grouped together (Mack+MD). Significant linear regressions between pCO_2 and pCH_4 are shown as lines that match legend entries by colour (* indicates $p < 0.05$).

When delta sites were examined across all sampling dates, the Peel River had a significantly greater excess of CO_2 relative to the atmosphere than any other site ($p < 0.05$), and was the only site to have consistently evasive fluxes across all dates (i.e., did not have a range that encompassed 0, or equilibrium with the atmosphere) (Fig. 3b). For CH_4, all sites had an excess relative to the atmosphere, although this excess was significantly greater in the outer delta ($p < 0.05$) (Fig. 3b). Values of pCO_2 and pCH_4 were significantly inversely related at the Mackenzie sites ($p < 0.05$) and in the outer delta ($p < 0.05$), but not in the Peel River (Fig. 5).

Inorganic carbon species as determinants of in situ gas concentrations

All channel sites in the Mackenzie Delta were found to be DIC-rich (Fig. 6a). Concentrations of DIC exceeded 1000 µmol L^{-1} on all sampling occasions, with average values over the freshet sampling period ranging from a low of 1615 µmol L^{-1} in the outer delta to a high of 1775 µmol L^{-1} in the Peel River. Concentrations of DIC were only significantly related to gas concentrations at the Mackenzie-influenced sites, however ($p < 0.01$ for both pCO_2 and pCH_4; Fig. 6a). Values for δ^{13}C-DIC fell in a narrow range, with average values during the freshet ranging from –6.14 to -6.52‰ in the Mackenzie sites and the Peel, respectively (Fig. 6b). The relationship between δ^{13}C-DIC and gas concentrations was not found to be significant at any site (Fig. 6b).

Instantaneous and delta-wide gas fluxes

In the Mackenzie River, values of F-CO_2 were below 0 mg-C m^{-2} d^{-1} throughout the rising freshet (Fig. 7a). Estimates of the average F-CO_2 during this period ranged from –258 mg-C m^{-2} d^{-1} to –112 mg-C m^{-2} d^{-1} (Table 1a), indicating a net invasion of CO_2 from the atmosphere into the river leading up to the highest-discharge period of the year. Following peak discharge on 19 May 2010, F-CO_2 values increased (Fig. 7a) and there was a net evasion of CO_2 from the Mackenzie River for the rest of the sampling period (low-high range in the estimated average F-CO_2 from 74 to 177 mg-C m^{-2} d^{-1}; Table 1a). Sites in the Mackenzie Delta that are strongly influenced by the Mackenzie River (Middle Channel, outer delta) also switched to net CO_2 invasion during the passage of peak discharge (Fig. 7a), while, in contrast, the Peel River remained a net emitter of CO_2 throughout the freshet (low-high range in the estimated average F-CO_2 from 373 to 871 mg-C m^{-2} d^{-1}; Table 1a). Net evasion of CH_4 was observed at all sites during the freshet, with F-CH_4 showing a strongly increasing trend throughout the sampling period at the outer delta sites (Fig. 7a). The average F-CO_2 value calculated across all sampling dates (F-CO_2) was greater in the Peel River than at any other site, while the average F-CH_4) value across all sampling dates was greatest in the

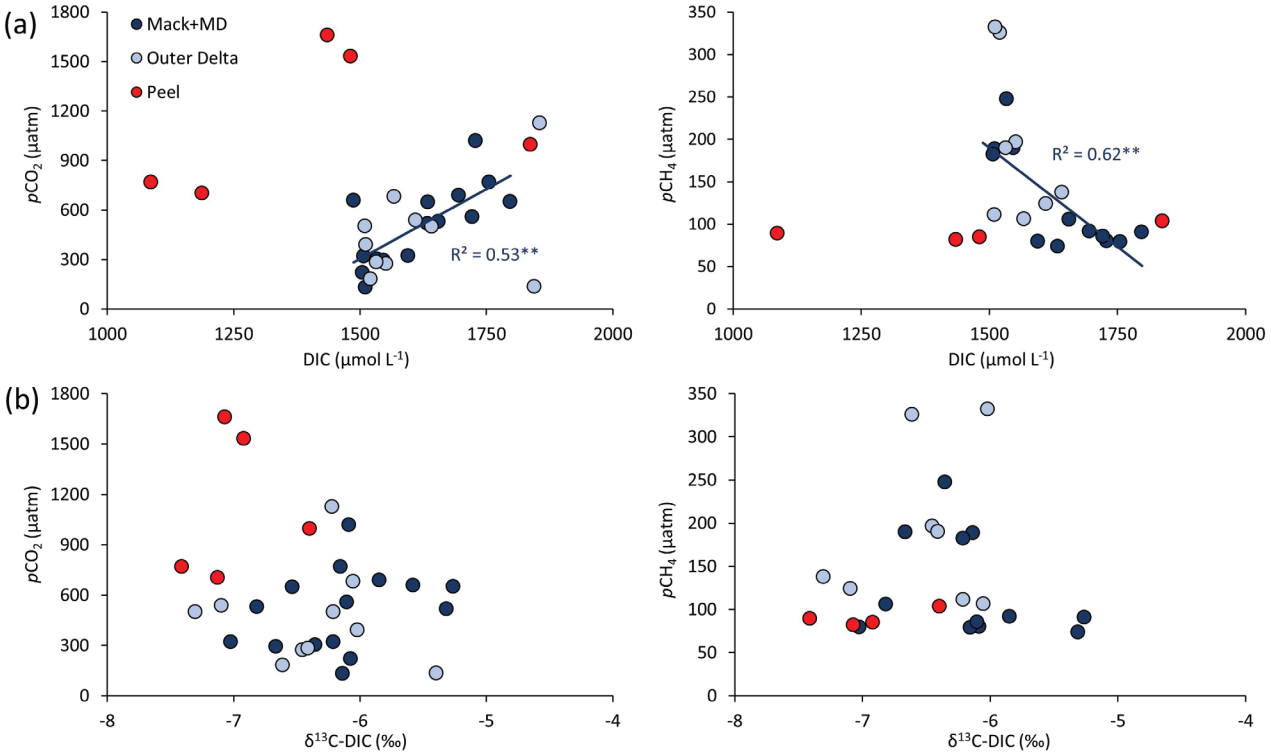

Fig. 6 Scatterplots of (a) DIC (µmol L^{-1}) and (b) δ^{13}C-DIC (expressed in per mille or ‰) versus pCO_2 (left) and pCH_4 (right). Note that the Mackenzie River and Middle Channel sites were grouped together (Mack+MD). Significant linear regressions are shown as lines that match legend entries by colour (** indicates $p < 0.01$).

outer delta (Fig. 7b). We only found a significant difference between the high (kCO_2 = 7 cm h^{-1}) and low (kCO_2 = 3 cm h^{-1}) estimates of average F-CO_2 in the Peel River; however, the high (kCH_4 = 6.90 cm h^{-1}) and low (kCH_4 = 2.96 cm h^{-1}) estimates of average F-CH_4 were significantly different at all sites (Fig. 7b).

Estimated gas fluxes from the entire Mackenzie Delta channel network are reported as high and low estimates that were calculated using gas concentration data and, respectively, the upper and lower limits on the gas transfer velocities that were proposed by Raymond & Cole (2001). For CO_2, the average instantaneous flux rate ranged (low to high) from 20.0 to 48.0 mg-C m^{-2} d^{-1} in the inflow transect, from 50.6 to 118.7 mg-C m^{-2} d^{-1} in the middle delta, and from 27.4 to 65.1 mg-C m^{-2} d^{-1} in the outer delta (Table 2a). For CH_4, flux rates ranged (low to high) from 2.6 to 6.1 mg-C m^{-2} d^{-1} in the inflow transect, 3.4 to 7.9 mg-C m^{-2} d^{-1} in the middle delta transect and 4.1 to 9.5 mg-C m^{-2} d^{-1} in the outer delta transect (Table 2b). When extrapolated across the total surface area of Mackenzie Delta channels throughout the month of May 2010, the total CO_2 flux was between 2.1 and 4.8 Gg-C, while the total CH_4 flux was between 186 and 433 Mg-C (Table 2). Excluding rising freshet data from delta-wide gas flux estimates had a greater effect on CO_2 fluxes than on CH_4 fluxes (Table 3). In the absence of rising freshet data, delta-wide CO_2 flux estimates were about 72% greater during the May 2010 freshet period, while CH_4 flux estimates were about 7% less. When extrapolated over the entire 2010 open-water period, which lasted from 25 April to 25 October, excluding rising freshet data increased delta-wide CO_2 flux estimates by 9% but decreased CH_4 flux estimates by only 2%.

Discussion

Unexpected freshet CO_2 gradients in the Mackenzie River and Delta

Although we expected to observe CO_2 supersaturation in the Mackenzie River during the freshet due to overwinter accumulation of dissolved gases under ice, we found that the Mackenzie was a net absorber of CO_2 during the ice-out and rising freshet periods of 2010. Most surprisingly, the lowest pCO_2 value (125 µatm) was observed on the day of peak flood (Fig. 3a). Our results countered prior observations in large seasonally flooded river systems, such as the Amazon (Richey et al. 2002; Rasera

Citation: *Polar Research* 2020, *39*, 3528, http://dx.doi.org/10.33265/polar.v39.3528

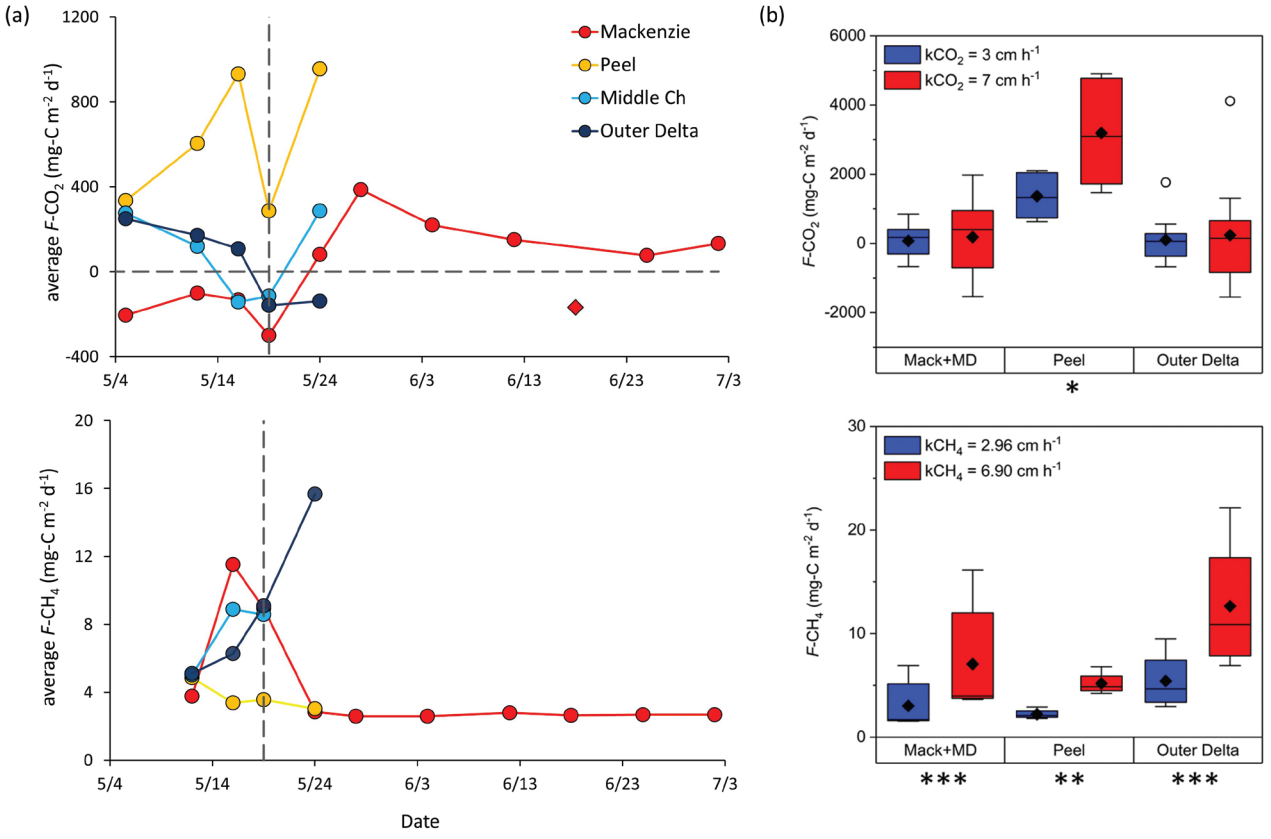

Fig. 7 Gas flux data for the Mackenzie River and Delta channels during the 2010 freshet. (a) Average *F*-GAS values (mg-C m^{-2} d^{-1}) for both CO_2 (top) and CH_4 (bottom), calculated as the average of our high and low estimates on each date. High and low estimates were derived using the upper and lower limits for the CO_2 gas transfer velocity (k_{CO2}) proposed by Raymond & Cole (2001). In all graphs, the dashed vertical line indicates the day of peak flood (19 May 2010), and the dashed horizontal line shown in the CO_2 graph denotes a flux of 0 mg-C m^{-2} d^{-1} (i.e., CO_2 equilibrium with the atmosphere). The red diamond in the pCO_2 graph denotes an anomalous data point (18 June 2010) that was excluded from all analyses. Note that there are no CH_4 data shown for the Middle Channel on 24 May 2010 because the sample was lost in transit. (b) *F*-GAS values for CO_2 (top) and CH_4 (bottom), calculated using daily gas concentration data and the lower (blue) and upper (red) limits on the gas-specific transfer velocity proposed by Raymond & Cole (2001). Note that the Mackenzie River and Middle Channel sites were considered together (Mack+MD). Boxplots show medians and quartiles (boxes), averages (filled diamonds), 90% confidence intervals (whiskers) and ranges (hollow dots). Paired *t*-tests were used to identify sites where the lower and upper limits on the gas transfer velocity produced significantly different average values of *F*-GAS (* indicates $p < 0.05$, ** indicates $p < 0.01$, *** indicates $p < 0.001$).

et al. 2013; Sawakuchi et al. 2017) and Mekong (Borges et al. 2018), which generally have the highest values of pCO_2 when water levels and discharge peak. In contrast to the Mackenzie, pCO_2 in the Peel River was consistently supersaturated throughout the rising freshet and peak discharge period (Table 1a, Fig. 3a). Our observations in the Peel more closely aligned with prior measurements in other north-flowing circumpolar rivers, such as the Kolyma (Semiletov 1999; Denfeld et al. 2013) and the Kuparuk (Kling et al. 1992), which tend to have supersaturated pCO_2 levels that are nevertheless substantially lower than those in tropical or temperate rivers (Table 1b).

Prior observations of CO_2 undersaturation in northern river systems have generally been restricted to small headwater streams, and to the summer low-water season. For example, in an extensive study of the Yukon River basin, Striegl et al. (2012) found that the average pCO_2 across all sampling sites was 1500 µatm, with most near- or below-equilibrium pCO_2 values measured in small headwater streams. Compared to larger streams and the river mainstem, headwater streams receive a disproportionately large amount of meltwater from ice and snow cover relative to their total discharge volume (Striegl et al. 2012), which dilutes concentrations of in situ CO_2. As another example, Denfeld et al. (2013) observed near-equilibrium pCO_2 values in the Kolyma River, which alternated between acting as a weak source and a weak sink of CO_2 (pCO_2 = 613 ± 315 µatm) during the summer open water period. The sampling

Table 2 Estimated fluxes of (a) CO_2 and (b) CH_4 across the air–water interface of Mackenzie Delta channels during the May 2010 freshet and ice-out. Values of *F*-GAS for each delta transect were calculated using gas concentration data and the low and high limits on the gas transfer velocity that were proposed by Raymond & Cole (2001). Values of *F*-GAS were then extrapolated across the channel surface area in each transect to give transect-specific fluxes, which were summed to give total delta-wide fluxes from all channel surfaces.

(a) CO_2	Inflow			Middle delta			Outer delta			Total flux (Gg-C)
	F-CO_2 (mg-C m^{-2} d^{-1})	area (km^2)	flux (Gg-C)	*F*-CO_2 (mg-C m^{-2} d^{-1})	area (km^2)	flux (Gg-C)	*F*-CO_2 (mg-C m^{-2} d^{-1})	area (km^2)	flux (Gg-C)	
Low limit (k_{CO2} = 3 cm h^{-1})	20.0	325.646	0.2	50.6	889.993	1.4	27.4	528.647	0.5	2.1
High limit (k_{CO2} = 7 cm h^{-1})	48.0	325.646	0.5	118.7	889.993	3.3	65.1	528.647	1.1	4.8

(b) CH_4	Inflow			Middle delta			Outer delta			Total flux (Mg-C)
	F-CH_4 (mg-C m^{-2} d^{-1})	area (km^2)	flux (Mg-C)	*F*-CH_4 (mg-C m^{-2} d^{-1})	area (km^2)	flux (Mg-C)	*F*-CH_4 (mg-C m^{-2} d^{-1})	area (km^2)	flux (Mg-C)	
Low limit (k_{CH4} = 2.96 cm h^{-1})	2.6	325.646	26.3	3.4	889.993	93.0	4.1	528.647	66.5	186
High limit (k_{CH4} = 6.90 cm h^{-1})	6.1	325.646	61.3	7.9	889.993	216.9	9.5	528.647	155.3	433

Table 3 Estimated delta-wide fluxes of (a) CO_2 (Gg-C) and (b) CH_4 (Mg-C) across the air–water interface of the Mackenzie Delta channel network. Estimates were calculated using the low and high limits on the gas transfer velocity that were proposed by Raymond & Cole (2001), and over both the month of May 2010 and the entire 2010 open water season (25 April–25 October 2010). The effect of including data from the rising freshet, which lasted from 25 April to 19 May 2010, was assessed by recalculating all flux estimates with rising freshet data from the inflow transect excluded.

	With rising freshet data	Rising freshet data excluded	% difference
(a) CO_2 (Gg-C)			
May 2010 (31 days)			
Low limit (k_{CO2} = 3 cm h^{-1})	2.1	3.5	173%
High limit (k_{CO2} = 7 cm h^{-1})	4.8	8.3	172%
2010 open-water season, 25 April – 25 October 2010 (183 days)			
Low limit (k_{CO2} = 3 cm h^{-1})	4.4	4.8	109%
High limit (k_{CO2} = 7 cm h^{-1})	10.4	11.3	109%
(b) CH_4 (Mg-C)			
May 2010 (31 days)			
Low limit (k_{CH4} = 2.96 cm h^{-1})	186	172	93%
High limit (k_{CH4} = 6.90 cm h^{-1})	433	401	93%
2010 open-water season, 25 April – 25 October 2010 (183 days)			
Low limit (k_{CH4} = 2.96 cm h^{-1})	772	759	98%
High limit (k_{CH4} = 6.90 cm h^{-1})	1801	1771	98%

period in Denfeld et al. (2013) was well after the full passage of the freshet in the Kolyma, when the dominant basin flow paths were through deeper soil layers rather than over the basin surface (Denfeld et al. 2013) where large amounts of dissolved gases are generated by aerobic and anaerobic decomposition. Unlike the DIC-rich Mackenzie system (flow-weighted concentrations greater than 20 mg L^{-1}; Tank et al. 2012; Gareis & Lesack 2017), the Kolyma is DIC-poor (flow-weighted concentration of 7.7 mg L^{-1}; Tank et al. 2012), which,

Citation: *Polar Research* 2020, *39*, 3528, http://dx.doi.org/10.33265/polar.v39.3528

along with primary production in basin surface waters, may have contributed to the periodic observations of pCO_2 undersaturation in the Kolyma (Denfeld et al. 2013). Large Subarctic and circumpolar rivers have not been hypothesized to be consistently undersaturated in CO_2 at any time of the year because of these few, specific instances that generate undersaturated pCO_2 conditions in this class of river.

Values of pCO_2 at downstream sites in the Mackenzie Delta also declined below atmospheric levels as the rising freshet progressed downstream, with the lowest pCO_2 values observed on 16 May in the middle delta and on 19 May in the outer delta (Fig. 3a). Again, these observations contradicted our expectation that overwinter accumulation of CO_2 under ice would generate supersaturated conditions during the freshet. Our results also contradicted prior observations in other floodplain systems around the world (Table 1b), which are generally strong direct sources of CO_2 to the atmosphere (Pulliam 1993; Richey et al. 2002; Marani & Alvalá 2007; Abril et al. 2014; Borges, Darchambeau et al. 2015) as well as sources of dissolved CO_2 to downstream regions because of high levels of the gas that are carried in floodwater (Borges, Darchambeau et al. 2015). During a prior study, late summer measurements of pCO_2 in an outer channel of the Mackenzie Delta averaged 694 µatm over a four-hour sampling period (Vallières et al. 2008), which aligned with our observed pCO_2 values in the Mackenzie River during the falling freshet (average = 581 µatm), implying that CO_2 levels in the Mackenzie may be consistently above atmospheric following the passage of peak flood. Overall, however, the Mackenzie Delta was only a weak emitter of CO_2 during the 2010 ice-out period.

It is unlikely that CO_2 undersaturation in the Mackenzie River and Delta during the freshet results from dilution by snowmelt, as was seen in the small headwater streams of the Yukon basin (Striegl et al. 2012). In the much larger Mackenzie River, the movement of snowmelt over the basin surface and through shallow sub-surface flow paths adds high levels of visibly chromophoric DOM. Absorption coefficients at 350 nm (a350), a proxy for DOM concentrations, reach an annual maximum of 14.6 m^{-1} during the rising freshet (Gareis 2018), as do concentrations of dissolved organic carbon (Gareis & Lesack 2017). These sources of dissolved organic material fuel CO_2-producing bacterial respiration following exposure to sunlight in surface waters (Cory et al. 2013). It is also unlikely that CO_2 undersaturation in the Mackenzie River and Delta results from in situ primary production, as was seen in the Kolyma during the summer low flow season (Denfeld et al. 2013). The Mackenzie River is extremely cold (average temperature < 1 °C; Gareis unpubl. data) and turbid (average total suspended solids concentration of 301 mg L^{-1}; Gareis & Lesack 2017) during the ice-out and freshet. Together, these conditions strongly limit rates of water-column primary production by both rooted and planktonic autotrophs during the rising freshet in the Mackenzie River, resulting in an average rising freshet chlorophyll concentration of 1.5 µg L^{-1} over the four years of this study (Gareis unpubl. data).

We propose that one plausible explanation for the observed CO_2 undersaturation in the Mackenzie River and Delta during the ice-out and freshet is a draw-down of CO_2 by the carbonate buffering system in the river. This would decrease the CO_2 concentration in water relative to that in air, thereby shifting the gradient across the air–water interface to favour CO_2 invasion while maintaining the high DIC concentrations observed in the river (Fig. 6a). The Mackenzie River contains high concentrations of carbonate particles (Brunskill 1986; Millot et al. 2003) that are generated by weathering of dolomite, calcite and other carbonate rocks in the high-relief Mackenzie and Rocky Mountains in the western Mackenzie basin and the flatter Interior Platform in the middle of the basin (Millot et al. 2003; Beaulieu, Goddéris et al. 2012). Furthermore, throughout the ice-out and freshet δ^{13}C-DIC fell in a narrow range (–5 to –8 ‰; Fig. 6b) that is characteristic of a geogenic source of inorganic carbon (Campeau et al. 2017) such as carbonate dissolution (Schulte et al. 2011), rather than the more isotopically light values (e.g., –26 to –28 ‰) that are generated when DIC is produced by the breakdown of organic matter (Coplen et al. 2002). Carbonate buffering resulting from chemical weathering of carbonate minerals in the river basin has been observed to decrease rates of CO_2 evasion in high-alkalinity systems (Stets et al. 2017) such as the Mackenzie (Tank et al. 2016). Chemical weathering consumed an estimated 9.2×10^{10} mol CO_2 a^{-1} in the Mackenzie River basin when atmospheric CO_2 concentrations were 355 µatm, with consumption projected to increase as atmospheric CO_2 increases in future (Beaulieu, Goddéris et al. 2012). Prior work on the Beaufort Shelf has found high concentrations of carbonate (4–5% by weight) in nearshore sediments, with concentrations decreasing as offshore distance from the Mackenzie Delta increases, supporting a riverine source of carbonate to the shelf (Pelletier 1975). Although these factors indicate that the carbonate buffering system is the most likely driver of CO_2 undersaturation in the Mackenzie during the rising freshet, further sampling during the ice-out and freshet periods is needed to definitively resolve this.

The Mackenzie River and Delta are strong emitters of CH_4 during the freshet

Contrary to our CO_2 results, our CH_4 results were consistent with our expectation that the Mackenzie River and Delta would remain a net source throughout the freshet and that concentrations and fluxes of CH_4 would be greatest around the time of peak water levels. Instantaneous rates of CH_4 flux in the Mackenzie Delta inflow rivers are comparable to, or somewhat lower than, many previously published values from other systems, with F-CH_4 in the Mackenzie ranging from 1.2 to 8.5 mg-C m^{-2} d^{-1} and in the Peel from 1.7 to 3.9 mg-C m^{-2} d^{-1}. For comparison, the average F-CH_4 in global circumpolar rivers is estimated to be 7 mg-C m^{-2} d^{-1} (Bastviken et al. 2011), while F-CH_4 was measured as 4 mg-C m^{-2} d^{-1} in the Kuparuk River (Kling et al. 1992) and 14.4 mg-C m^{-2} d^{-1} in the Yukon (Striegl et al. 2012) (Table 1). Our results therefore align with the results of prior studies of CH_4 in northern rivers (Bastviken et al. 2011) as well as rivers and streams worldwide (Stanley et al. 2016), which have shown that CH_4 supersaturation and evasion to the atmosphere are the norms in lotic systems.

A large net excess of CH_4 gas (Fig. 3b) and strong evasive fluxes to the atmosphere (Fig. 7) were observed at all downstream sites in the Mackenzie Delta. Values of $p$$CH_4$ in the outer delta transect were supersaturated (average 189 µatm) and comparable to reported $p$$CH_4$ values in the Kuparuk River in Alaska (236 µatm; Kling et al. 1992), as well those for river floodplains at lower latitudes (see examples in Table 1b). Our results were in agreement with two prior studies that were conducted for other large circumpolar river deltas. In a 10-year study in the Yukon River system, all sampled locations (240+) were found to be supersaturated with CH_4 (Striegl et al. 2012), while in the Lena, sampling sites in the river mainstem and delta channels were between 900% and 3000% supersaturated with CH_4 (Bussmann 2013).

Our CH_4 results are therefore comparable to previously published CH_4 concentrations and fluxes in other large circumpolar rivers and deltas, and align with our hypothesis that the greatest gas fluxes would be observed at downstream sites in the delta. The increasing rates of CH_4 evasion we saw in the middle and outer delta as the freshet progressed downstream may have been subsidized by dissolved CH_4 from floodplain lakes on the Mackenzie Delta. At ice-out, delta lakes are supersaturated with CH_4 due to overwinter accumulation under ice, with concentrations of up to 1050 mg-C m^2 (Cunada 2016). As water levels reach their peak, an average of 25.8 km^3 of floodwater spreads out over the Mackenzie Delta floodplain, where it mixes with up to 5.4 km^3 of CH_4-supersaturated lake water (Emmerton et al. 2007). This modified mixture of floodwater and lake water drains back into delta channels, where it has the potential to reinforce the CH_4 peak seen in the Mackenzie River and drive the large excess of CH_4 in water relative to air that was observed at downstream sites.

Factors affecting gas flux estimates

To our knowledge, this study presents the first direct measurements of CO_2 and CH_4 concentrations during the ice-out and rising freshet periods in a large north-flowing circumpolar river delta. Although gas concentrations in water and the overlying atmosphere are straightforward to measure, the calculation of accurate gas transfer velocities is far more difficult, and inaccuracies in k_{600} values can result in large errors in instantaneous and system-wide fluxes. There are therefore two factors that may have produced errors in our k_{600} values, and subsequently our gas flux estimates, which must be considered when interpreting the results of this study.

The first is that we used a method of calculating k_{600} that was derived from the literature, rather than from repeated measurements of gas concentrations in a closed system at the air–water interface (the "floating chamber" method, as described by Frankignoulle [1988]). Although applying generalized gas transfer velocities from the literature can produce significant errors in estimates of flux rates (e.g., as discussed by Wallin et al. 2011), we were unable to use the floating chamber method to calculate system-specific flux rates because of the sampling conditions during the ice-out period when our study took place. Our objective was to quantify CO_2 and CH_4 concentrations and fluxes during ice-out and the high-discharge period of the rising freshet leading up to peak flood, when ice in delta channels has fractured and started to move downstream with increasing speed and force driven by rapidly increasing discharge. The only way to access sampling sites during this time is by means of a helicopter, which requires either landing on ice sheets or sampling off the helicopter pontoons in mid-channel openings in the ice cover. This constrained our sampling to only direct measurements of gas concentrations in channels, and we therefore inferred the direction of gas flow throughout the ice-out and high-discharge freshet period using concentration gradients across the air–water interface.

Although our sampling method accurately resolved the direction of the gas flux, the gas exchange coefficients we used to calculate fluxes undoubtedly influenced our results. The gas exchange coefficient (k_{600}) is an expression of the turbulent energy at the air–water interface, and both its value and its variability within a system are important determinants of gas flux rates (Raymond & Cole 2001; Alin et al. 2011; Striegl et al. 2012; Raymond et al. 2013; Sawakuchi et al. 2017). In

Citation: *Polar Research* 2020, *39*, 3528, http://dx.doi.org/10.33265/polar.v39.3528

shallower streams and headwaters, k_{600} is controlled by bottom friction and is generally a function of water current velocity and channel slope (Alin et al. 2011; Raymond et al. 2012). At larger scales, such as in estuaries and river mainstems greater than 100 m in width, wind exerts a stronger influence on k_{600} values (Raymond & Cole 2001; Alin et al. 2011). Additionally, there are other factors that may also influence gas transfer velocities in the Mackenzie River and Delta during breakup, including increased roughness of the air–water interface due to ice rubble and debris in the channel, ice jams in delta channels that increase the lateral spread of floodwater onto the floodplain, and wind and water currents that are directionally opposed to one another (Zappa et al. 2007; Beaulieu, Shuster et al. 2012). In the absence of direct measurements of k_{600} across the air–water interface in Mackenzie Delta channels and, after consideration of potential extreme gas coefficient values in this system (see the Supplementary material), we have opted to present estimates of instantaneous gas fluxes that were generated using the limits proposed by Raymond & Cole (2001). However, given that all river and delta channels that were sampled during this study were considerably wider than 100 m (ranging from approximately 300 m to over 4 km in width), and that wind speeds can be high in the area (particularly along the Beaufort coast), the fluxes presented herein are likely conservative estimates and we acknowledge that actual fluxes of both CO_2 and CH_4 are likely much greater.

The second factor that must be considered is that our sampling programme was restricted to delta channels and did not include samples from wetted floodplain surfaces that were covered by some amount of river water during the freshet. Floodplains are substantial sources of CO_2 and CH_4 evasion in other systems (Pulliam 1993; Richey et al. 2002; Marani & Alvalá 2007; Abril et al. 2014; Borges, Darchambeau et al. 2015; Dalmagro et al. 2018) due to leaching of gases from submerged soils and vegetation, and both aerobic and anaerobic decomposition of organic matter. Although we were unable to sample directly over wetted floodplain surfaces, our sampling scheme included downstream locations in the outer delta, and data from these sites suggest that there may be significant contributions of CH_4 that are generated on the delta floodplain. Also, during high-water periods, the more than 45 000 floodplain lakes on the Mackenzie Delta become hydrologically reconnected to delta channels. Prior work in these floodplain lakes (Tank et al. 2009; Cunada 2016) suggests that large amounts of dissolved gases generated under ice over winter may be mobilized into distributary channels when lakes are flooded during the freshet. Accurate quantification of these potentially significant fluxes of carbon-based greenhouse gases over seasonally flooded portions of the Mackenzie Delta floodplain will require further study.

Delta-wide estimates of freshet and open water gas fluxes

We estimated the total ice-out gas fluxes from the Mackenzie Delta by combining our low and high estimates for the Mackenzie Delta channels (2.1 to 4.8 Gg-C as CO_2, 186 and 433 Mg-C as CH_4; Table 2) with previously published ice-out fluxes for the more than 45 000 floodplain lakes in the Mackenzie Delta. For CO_2, our channel flux estimate is comparable in magnitude to the ice-out flux estimate for Mackenzie Delta floodplain lakes (10.6 Gg-C as CO_2; Cunada 2016), but for CH_4 our channel flux estimate is an order of magnitude lower than that for Mackenzie Delta floodplain lakes (8.41 Gg-C as CH_4; Cunada 2016). Together, our fluxes along with those of Cunada (2016) suggest that between 12.7 and 15.4 Gg-C evades from the Mackenzie Delta as CO_2 during ice out, and between 8.6 and 8.8 Gg-C evades as CH_4. These are the first estimates of the fluxes of CO_2 and CH_4 from a large circumpolar river delta during ice-out of which we are aware.

Delta-wide flux estimates of CO_2 were more greatly affected by the exclusion of rising freshet data than were CH_4 flux estimates (Table 3), reflecting the switch from net invasion to evasion of CO_2 with the passage of peak flood in the Mackenzie River and Delta. Although the difference between the CO_2 flux estimates with and without rising freshet data was large during the May 2010 ice-out period (ca. 72%), the short duration of the rising freshet (24 days) relative to the rest of the open water period (153 days) means that there was only a moderate difference (ca. 9%) between the two total open water season flux estimates. These results are based on data from only a single ice-out and breakup period, however, and may therefore either under- or overestimate the effect of temporary CO_2 undersaturation on total delta-wide fluxes. Sampling during future ice-out and breakup periods is needed to resolve the magnitude of the effect of CO_2 drawdown on fluxes in this system.

Conclusions

While fluxes of CO_2 and CH_4 from large rivers in the tropics and temperate zones are relatively well known, they are poorly characterized and may be underestimated in large river systems at high latitudes (e.g., Bastviken et al. 2011; Raymond et al. 2013). Fluxes of two globally-important greenhouse gases across the air–water interface were monitored in the channel network of the Mackenzie Delta during the ice-out and freshet periods of 2010,

which corresponds with the ice-out period for the more than 45 000 floodplain lakes in this exceptionally lake-rich system. This study is the first of which we are aware which quantified CO_2 and CH_4 during the historically under-sampled periods of ice-out, rising freshet and peak water levels in one of the world's major circumpolar rivers and its delta.

We conservatively estimated that total fluxes from the channel network for the month of May 2010 were 2.1–4.8 Gg-C as CO_2, and 186–433 Mg-C as CH_4. While the Peel River was a strong net emitter of CO_2 throughout the freshet, it contributes a relatively small proportion of the total water flow into the delta (ca. 5%), with most inflowing water (ca. 95%) coming from the Mackenzie River. The Mackenzie was a net absorber of CO_2 during the rising freshet (F-CO_2 of -112 to -258 mg-C m^{-2} d^{-1}), as were downstream sites in the delta, with all sites switching to CO_2 evasion around the time of peak flood and water levels. Overall, the Mackenzie Delta was a weak emitter of CO_2 during the 2010 ice-out and freshet, which was unexpected and contradicts observations in other large river systems where high evasive fluxes of CO_2 are observed during high-flow periods. All sites were strong emitters of CH_4 throughout the freshet and ice-out, however, with upstream–downstream concentration gradients that suggest that the delta floodplain is a source of this gas.

Current estimates of gas evasion from global rivers are 1.8 Pg-C a^{-1} as CO_2 (Raymond et al. 2013) and 20.1 Tg-C a^{-1} as CH_4 (Stanley et al. 2016). Although Mackenzie Delta ice-out fluxes represent only a very small percentage of the total annual global flux for either gas, our results nevertheless provide critical information that can be used to refine estimates of gas fluxes from high-latitude lotic systems during the relatively under-studied ice-out and freshet periods. However, our results also point towards a need for repeated sampling in future years to determine whether the CO_2 undersaturation observed during the 2010 freshet is a yearly occurrence in the Mackenzie, and to determine the mechanism responsible for this seasonal draw-down of CO_2 in one of the world's largest circumpolar river delta systems.

Acknowledgements

The research reported in this article was conducted under NWT Scientific Research Licence no. 14 687. Logistical support was provided by the Aurora Research Institute and the Inuvik Office of the Water Survey of Canada branch of Environment Canada. Analytical support was provided by the laboratories of V.L. St. Louis (University of Alberta) and C.L. Osburn (North Carolina State University). The authors thank C.L. Cunada for valuable help with methods, L. Duma for assistance in the field and laboratory and R.W. Macdonald for suggestions and comments that greatly improved the manuscript. Three anonymous reviewers also provided suggestions and comments that greatly improved the quality of this article.

Disclosure statement

The authors report no conflict of interest.

Funding

Funding for this study was provided by the Government of Canada International Polar Year project Study of Canadian Arctic River-delta Fluxes, the Natural Sciences and Engineering Research Council of Canada (Discovery Grant to LFWL, Northern Research Internship to JALG), the Polar Continental Shelf Program, the Northern Scientific Training Program and the Aurora Research Institute.

References

Abril G., Martinez J.M., Artigas L.F., Moreira-Turcq P., Benedetti M.F., Vidal L., Meziane T., Kim J.H., Bernardes M.C., Savoye N., Deborde J., Souza E.L., Alberic P., de Souza M.F.L. & Roland F. 2014. Amazon river carbon dioxide outgassing fueled by wetlands. *Nature 505*, 395–398, doi: 10.1038/nature12797.

Alin S.R., Rasera M.F.F.L., Salimon C.I., Richey J.E., Holtgrieve G.W., Krusche A.V. & Snidvongs A. 2011. Physical controls on carbon dioxide transfer velocity and flux in low-gradient river systems and implications for regional carbon budgets. *Journal of Geophysical Research—Biogeosciences 116*, G01009, doi: 10.1029/2010JG001398.

Alt D.F. 1993. *State water data records: hydrologic records of the United States water years 1990, 1991 and 1992. United States Geological Survey Open File Report 93-626*. CD-ROM. Doi: 10.3133/ofr93626. US Geological Survey.

Amon R.M.W., Rinehart A.J., Duan S., Louchouarn P., Prokushkin A., Guggenberger G., Bauch D., Stedmon C., Raymond P.A., Holmes R.M, McClelland J.W., Peterson B.J., Walker S.A. & Zhulidov A.V. 2012. Dissolved organic matter sources in large Arctic rivers. *Geochimica et Cosmochimica Acta 94*, 217–237, doi: 10.1016/j.gca.2012.07.015.

Bastviken D., Tranvik L.J., Downing J.A., Crill P.M. & Enrich-Prast A. 2011. Freshwater methane emissions offset the continental carbon sink. *Science 331*, 50, doi: 10.1126/science.1196808.

Beaulieu E., Goddéris Y., Donnadieu Y., Labat D. & Roelandt C. 2012. High sensitivity of the continental-weathering carbon dioxide sink to future climate change. *Nature Climate Change 2*, 346–349, doi: 10.1038/nclimate1419.

Beaulieu J.J., Shuster W.D. & Rebholz J.A. 2012. Controls on gas transfer velocities in a large river. *Journal of Geophysical Research—Biogeosciences 117*, G02007, doi: 10.1029/2011jg001794.

Beltaos S. 2012. Mackenzie Delta flow during spring breakup: uncertainties and potential improvements. *Canadian Journal of Civil Engineering 39*, 579–588, doi: 10.1139/I2012-033.

Blackburn J., She Y., Hicks F. & Nafziger J. 2015. Ice effects on flow distributions in the Mackenzie Delta. *Proceedings of the 18th Workshop on the Hydraulics of Ice Covered Rivers*. Quebec City: Committee on River Ice Processes and the Environment.

Borges A.V., Abril G. & Bouillon S. 2018. Carbon dynamics and CO_2 and CH_4 outgassing in the Mekong delta. *Biogeosciences 15*, 1093–1114, doi: 10.5194/bg-15-1093-2018.

Borges A.V., Abril G., Darchambeau F., Teodoru C.R., Deborde J., Vidal L.O., Lambert T. & Bouillon S. 2015. Divergent biophysical controls of aquatic CO_2 and CH_4 in the world's two largest rivers. *Scientific Reports 5*, article no. 15614, doi: 10.1038/srep15614.

Borges A.V., Darchambeau F., Teodoru C.R., Marwick T.R., Tamooh F., Geeraert N., Omengo F.O., Guerin F., Lambert T., Morana C., Okuku K. & Bouillon S. 2015. Globally significant greenhouse-gas emissions from African inland waters. *Nature Geoscience 8*, 637–642, doi: 10.1038/ngeo2486.

Brunskill G.J. 1986. Environmental features of the Mackenzie System. In B.R. Davies & K.F. Walker (eds.): *The ecology of river systems*. Pp. 435–471. Dordrecht: Dr. W. Junk Publishers.

Bussmann I. 2013. Distribution of methane in the Lena Delta and Buor-Khaya Bay, Russia. *Biogeosciences 10*, 4641–4652, doi: 10.5194/bg-10-4641-2013.

Bussmann, I., Hackbusch S., Schaal P. & Wichels A. 2017. Methane distribution and oxidation around the Lena Delta in summer 2013. *Biogeosciences 14*, 4985–5002, doi: 10.5194/bg-14-4985-2017.

Butman D. & Raymond P.A. 2011. Significant efflux of carbon dioxide from streams and rivers in the United States. *Nature Geoscience 4*, 839–842, doi: 10.1038/ngeo1294.

Campeau A. & Del Giorgio P.A. 2014. Patterns in CH_4 and CO_2 concentrations across boreal rivers: major drivers and implications for fluvial greenhouse gas emissions under climate change scenarios. *Global Change Biology 20*, 1075–1088, doi: 10.1111/gcb.12479.

Campeau A., Wallin M.B., Giesler R., Löfgren S., Mörth C.-M., Schiff S., Venkiteswaran J.J. & Bishop K. 2017. Multiple sources and sinks of dissolved inorganic carbon across Swedish streams, refocusing the lens of stable C isotopes. *Scientific Reports 7*, article no. 9158, doi: 10.1038/s41598-017-09049-9.

Cole J.J. & Caraco N.F. 2001. Carbon in catchments: connecting terrestrial carbon losses with aquatic metabolism. *Freshwater and Marine Research 52*, 101–110, doi: 10.1071/MF00084.

Coplen T.B., Hopple J.A., Böhlke J.K., Peiser H.S., Rieder S.E., Krouse H.R., Rosman K.J.R., Ding T., Vocke R.D. Jr. Révész K.M., Lamberty A., Taylor P. & De Bièvre P. 2002. *Compilation of minimum and maximum isotope ratios of selected elements in naturally occurring terrestrial materials and reagents*. *Water-Resources Investigations Report 01-4222*. Reston, VA: US Department of the Interior and US Geological Survey.

Cory R.M., Crump B.C., Dobkowski J.A. & Kling G.W. 2013. Surface exposure to sunlight stimulates CO_2 release from permafrost soil carbon in the Arctic. *Proceedings of the National Academy of Sciences of the United States of America 110*, 3429–3434, doi: 10.1073/pnas.1214104110.

Crawford J.T., Striegl R.G., Wickland K.P., Dornblaser M.M. & Stanley E.H. 2013. Emissions of carbon dioxide and methane from a headwater stream network of interior Alaska. *Journal of Geophysical Research—Biogeosciences 118*, 482–494, doi: 10.1002/jgrg.20034.

Cunada C.L. 2016. *Seasonal methane dynamics in lakes of the Mackenzie river delta, western Canadian Arctic*. MSc thesis, Simon Fraser University.

Dalmagro H.J., Lathuilliere M.J., Hawthorne I., Morais D.D., Pinto O.B., Couto E.G. & Johnson M.S. 2018. Carbon biogeochemistry of a flooded Pantanal forest over three annual flood cycles. *Biogeochemistry 139*, 1–18, doi: 10.1007/s10533-018-0450-1.

Denfeld B.A., Frey K.E., Sobczak W.V., Mann P.J. & Holmes R.M. 2013. Summer CO_2 evasion from streams and rivers in the Kolyma river basin, north-east Siberia. *Polar Research 32*, article no. 19704, doi: 10.3402/polar.v32i0.19704.

Denfeld B.A., Wallin M.B., Sahlée E., Sobek S., Kokic J., Chmiel H.E. & Weyhenmeyer G.A. 2015. Temporal and spatial carbon dioxide concentration patterns in a small boreal lake in relation to ice-cover dynamics. *Boreal Environment Research 20*, 679–692.

Dlugokencky E.J., Crotwell A.M. & Mund J.W. 2019. Atmospheric methane dry air mole fractions from quasi-continuous measurements at Barrow, Alaska and Mauna Loa, Hawaii, 1986-2018. Version 2019-03-04. Accessed on the internet at ftp://aftp.cmdl.noaa.gov/data/trace_gases/ch4/in-situ/surface/ on 20 January 2020.

Emmerton C.A., Lesack L.F.W. & Marsh P. 2007. Lake abundance, potential water storage, and habitat distribution in the Mackenzie river delta, western Canadian Arctic. *Water Resources Research 43*, W05419, doi: 10.1029/2006WR005139.

EPA (Environmental Protection Agency) 2004. *Standard operating procedure. Sample preparation and calculations for dissolved gas analysis in water samples using a gc headspace equilibration technique. RSKSOP-175. 2004. Revision 2.* Accessed on the internet at https://archive.epa.gov/region1/info/testmethods/web/pdf/rsksop175v2.pdf on 16 January 2020.

Frankignoulle M. 1988. Field measurements of air–sea CO_2 exchange. *Limnology and Oceanography 33*, 313–322, doi: 10.4319/lo.1988.33.3.0313.

Gan W.B., Chen H.M. & Hart Y.F. 1983. Carbon transport by the Yangtze (at Nanjing) and Huanghe (at Jinan) rivers, People's Republic of China. In E.T. Degens et al. (eds.): *Transport of carbon and minerals in major world rivers. Part 2*. Pp. 459–470. Hamburg: Scientific Committee on Problems of the Environment, United Nations Environment Programme.

Gareis J.A.L. 2018. *Arctic deltas as biogeochemical hotspots affecting the delivery of nutrients and dissolved organic matter to the Arctic Ocean*. PhD thesis, Simon Fraser University.

Gareis J.A.L. & Lesack L.F.W. 2017. Fluxes of particulates and nutrients during hydrologically defined seasonal periods in an ice-affected great Arctic river, the Mackenzie. *Water Resources Research 53*, 6109–6132, doi: 10.1002/2017WR020623.

Gran G. 1952. Determination of the equivalence point in potentiometric titrations, part II. *Analyst 77*, 661–671, doi: 10.1039/AN9527700661.

Hamilton J.D., Kelly C.A., Rudd J.W.M., Hesslein R.H. & Roulet N.T. 1994. Flux to the atmosphere of CH_4 and CO_2 from wetland ponds on the Hudson Bay Lowlands (HBLs). *Journal of Geophysical Research—Atmospheres 99*, 1495–1510, doi: 10.1029/93JD03020.

Hesslein R.H., Rudd J.W.M., Kelly C., Ramlal P. & Hallard K.A. 1991. Carbon dioxide pressure in surface waters of Canadian lakes. In S.C. Wilhelms & J.S. Gulliver (eds.): *Air–water mass transfer: selected papers from the second international symposium on gas transfer at water surfaces*. Pp 413–431. New York, NY: American Society of Civil Engineers.

HYDAT 2019. Water Survey of Canada real time hydrometric data. Accessed on the internet https://wateroffice.ec.gc.ca/search/historical_e.html on 16 January 2020.

Jammet M., Dengel S., Kettner E., Parmentier F.J.W., Wik M., Crill P. & Friborg T. 2017. Year-round CH_4 and CO_2 flux dynamics in two contrasting freshwater ecosystems of the Subarctic. *Biogeosciences 14*, 5189–5216, doi: 10.5194/bg-14-5189-2017.

Kling G.W., Kipphut G.W. & Miller M.C. 1992. The flux of CO_2 and CH_4 from lakes and rivers in Arctic Alaska. *Hydrobiologia 240*, 23–36, doi: 10.1007/BF00013449.

Lauerwald R., Laruelle G.G., Hartmann J., Ciais P. & Regnier P.A. 2015. Spatial patterns in CO_2 evasion from the global river network. *Global Biogeochemical Cycles 29*, 534–554, doi: 10.1002/2014GB004941.

Lesack L.F.W. & Marsh P. 2010. River-to-lake connectivities, water renewal, and aquatic habitat diversity in the Mackenzie River Delta. *Water Resources Research 46*, W12504, doi: 10.1029/2010WR009607.

Lesack L.F.W., Marsh P., Hicks F.E. & Forbes D.L. 2013. Timing, duration, and magnitude of peak annual water levels during ice breakup in the Mackenzie Delta and the role of river discharge. *Water Resources Research 49*, 8234–8249, doi: 10.1002/2012WR013198.

MacIntyre S., Wanninkhof R. & Chanton J.P. 1995. Trace gas exchange across the air–water interface in freshwater and coastal marine environments. In P.A. Matson & R.C. Harriss (eds.): *Biogenic trace gases: measuring emissions from soil and water*. Pp. 52–97. Oxford: John Wiley and Sons Ltd.

Marani L. & Alvalá P.C. 2007. Methane emissions from lakes and floodplains in Pantanal, Brazil. *Atmospheric Environment 41*, 1627–1633, doi: 10.1016/j.atmosenv.2006.10.046.

Michmerhuizen C.M., Striegl R.G. & McDonald M.E. 1996. Potential methane emission from north-temperate lakes following ice melt. *Limnology and Oceanography 41*, 985–991, doi: 10.4319/lo.1996.41.5.0985.

Millot R., Gaillardet J., Dupré B. & Allègre C.J. 2003. Northern latitude chemical weathering rates: clues from the Mackenzie river Basin, Canada. *Geochimica et Cosmochimica Acta 67*, 1305–1329, doi: 10.1016/S0016-7037(02)01207-3.

Morley J.K.A. 2012. *Observations of flow distributions and river breakup in the Mackenzie Delta, NWT*. MSc thesis, University of Alberta.

NOAA ESRL Global Monitoring Division 2016, updated annually. Atmospheric carbon dioxide dry air mole fractions from quasi-continuous measurements at Barrow, Alaska. Version 2017-8. Compiled by K.W. Thoning et al. Doi: 10.7298/V5RR1W6B. Boulder, CO: National Oceanic and Atmospheric Administration, Earth System Research Laboratory, Global Monitoring Division.

Osburn C.L. & St-Jean G. 2007. The use of wet chemical oxidation with high-amplification isotope mass spectrometry (WCO-IRMS) to measure stable isotope values of dissolved organic carbon in seawater. *Limnology and Oceanography—Methods 5*, 296–308, doi: 10.4319/lom.2007.5.296.

Pelletier B.R. 1975. *Sediment dispersal in the southern Beaufort Sea (Beaufort Sea Technical Report 25a)*. Victoria, Canada: Beaufort Sea Project.

Phelps A.R., Peterson K.M. & Jeffries M.O. 1998. Methane efflux from high-latitude lakes during spring ice melt. *Journal of Geophysical Research—Atmospheres 103*, 29029–29036, doi: 10.1029/98JD00044.

Pulliam W.M. 1993. Carbon dioxide and methane exports from a southeastern floodplain swamp. *Ecological Monographs 63*, 29–53, doi: 10.2307/2937122.

Rasera M.F.F.L., Krusche A.V., Richey J.E., Ballester M.V.R. & Victória R.L. 2013. Spatial and temporal variability of pCO_2 and CO_2 efflux in seven Amazonian rivers. *Biogeochemistry 116*, 241–259, doi: 10.1007/s10533-013-9854-0.

Raymond P.A., Caraco N.F. & Cole J.J. 1997. Carbon dioxide concentration and atmospheric flux in the Hudson river. *Estuaries 20*, 381–390, doi: 10.2307/1352351.

Raymond P.A. & Cole J.J. 2001. Gas exchange in rivers and estuaries: choosing a gas transfer velocity. *Estuaries 24*, 312–317, doi: 10.2307/1352954.

Raymond P.A., Hartmann J., Lauerwald R., Sobek S., McDonald C., Hoover M., Butman D., Striegl R., Mayorga E., Humborg C., Kortelainen P., Dürr H., Meybeck M., Ciais P. & Guth P. 2013. Global carbon dioxide emissions from inland waters. *Nature 503*, 355–359, doi: 10.1038/nature12760.

Raymond P.A., Zappa C.J., Butman D., Bott T.L., Potter J., Mulholland P., Laursen A.E., McDowell W.H. & Newbold D. 2012. Scaling the gas transfer velocity and hydraulic geometry in streams and small rivers. *Limnology and Oceanography: Fluids and Environments 2*, 41–53, doi: 10.1215/21573689-1597669.

Richey J.E., Melack J.M., Aufdenkampe A.K., Ballester V.M. & Hess L.L. 2002. Outgassing from Amazonian rivers and wetlands as a large tropical source of atmospheric CO_2. *Nature 416*, 617–620, doi: 10.1038/416617a.

Sander R. 2014. Compilation of Henry's Law constants, version 3.99. *Atmospheric Chemistry and Physics Discussions 14*, 29615–30521, doi: 10.5194/acpd-14-29615-2014.

Sawakuchi H.O., Neu V., Ward N.D., Barros M.dL.C, Valerio A.M., Gagne-Maynard W., Cunha A.C., Less D.F.S., Diniz J.E.M., Brito D.C., Krusche A.V. & Richey J.E. 2017. Carbon dioxide emissions along the lower Amazon river. *Frontiers in Marine Science 4*, UNSP 76, doi: 10.3389/fmars.2017.00076.

Schulte P., van Geldern R., Freitag H., Karim A., Négrel P., Petelet-Giraud E., Probst A., Probst J.-L., Telmer K., Veizer J. & Barth J.A.C. 2011. Applications of stable water and carbon isotopes in watershed research: weathering, carbon cycling, and water balances. *Earth-Science Reviews 109*, 20–31, doi: 10.1016/j.earscirev.2011.07.003.

Semiletov I.P. 1999. Aquatic sources and sinks of CO_2 and CH_4 in the polar regions. *Journal of the Atmospheric Sciences 56*, 286–306, doi: 10.1175/1520-0469(1999)056<0286:ASASOC>2.0.CO;2.

Spencer R.G.M., Mann P.J., Dittmar T., Eglinton T.I., Mcintyre C., Holmes R.M., Zimov N. & Stubbins A. 2015. Detecting the signature of permafrost thaw in Arctic rivers. *Geophysical Research Letters 42*, 2830–2835, doi: 10.1002/2015GL063498.

Stanley E.H., Casson N.J., Christel S.T., Crawford J.T., Loken L.C. & Oliver S.K. 2016. The ecology of methane in streams and rivers: patterns, controls, and global significance. *Ecological Monographs 86*, 146–171, doi: 10.1890/15-1027.

Stets E.G.D., Butman D., McDonald C.P., Stackpoole S.M., DeGrandpre M.D. & Striegl R.G. 2017. Carbonate buffering and metabolic controls on carbon dioxide in rivers. *Global Biogeochemical Cycles 31*, 663–677, doi: 10.1002/2016GB005578.

Striegl R.G., Dornblaser M.M., McDonald C.P., Rover J.R. & Stets E.G. 2012. Carbon dioxide and methane emissions from the Yukon river system. *Global Biogeochemical Cycles 26*, GB0E05, doi: 10.1029/2012GB004306.

Tank S.E., Lesack L.F.W. & Hesslein R.H. 2009. Northern delta lakes as summertime CO_2 absorbers within the Arctic landscape. *Ecosystems 12*, 144–157, doi: 10.1007/s10021-008-9213-5.

Tank S.E., Raymond P.A., Striegl R.G., McClelland J.W., Holmes R.M., Fiske G.J. & Peterson B.J. 2012. A land-to-ocean perspective on the magnitude, source and implication of DIC flux from major Arctic rivers to the Arctic Ocean. *Global Biogeochemical Cycles 26*, GB4018, doi: 10.1029/2011GB004192.

Tank S.E., Striegl R.G., McClelland J.W. & Kokelj S.V. 2016. Multi-decadal increases in dissolved organic carbon and alkalinity flux from the Mackenzie drainage basin to the Arctic Ocean. *Environmental Research Letters 11*, 054015, doi: 10.1088/1748-9326/11/5/054015.

Telang S.A. 1985. Transport of carbon and minerals in the Mackenzie river. In E.T. Degens et al. (eds.): *Transport of carbon and minerals in major world rivers. Part 3*. Pp. 337–344. Hamburg: *Scientific Committee* on Problems of the Environment, United Nations Environment Programme.

Vallières C., Retamal L., Ramlal P., Osburn C.L. & Vincent W.F. 2008. Bacterial production and microbial food web structure in a large Arctic river and the coastal Arctic Ocean. *Journal of Marine Systems 74*, 756–773, doi: 10.1016/j.jmarsys.2007.12.002.

Vonk J.E., Mann P.J., Davydov S., Davydova A., Spencer R.G.M., Schade J., Sobczak W.V., Zimov N., Zimov S., Bulygina E., Eglinton T.I. & Holmes R.M. 2013. High biolability of ancient permafrost carbon upon thaw. *Geophysical Research Letters 40*, 2689–2693, doi: 10.1002/grl.50348.

Wallin M., Buffam I., Öquist M., Laudon H. & Bishop K. 2010. Temporal and spatial variability of dissolved inorganic carbon in a boreal stream network, concentration and downstream evasion. *Journal of Geophysical Research—Biogeosciences 115*, GO2014, doi: 10.1029/2900JG001100.

Wallin M., Öquist M., Buffam I., Billett M., Nisell J. & Bishop K. 2011. Spatiotemporal variability of the gas transfer coefficient (K_{CO2}) in boreal streams: implications for large scale estimates of CO_2 evasion. *Global Biogeochemical Cycles 25*, GB3025, doi: 10.1029/2010GB003975.

Wanninkhof R. 1992. Relationship between wind speed and gas exchange over the ocean. *Journal of Geophysical Research—Oceans 97*, 7373–7382, doi: 10.1029/92JC00188.

Wanninkhof R. & Knox M. 1996. Chemical enhancement of CO_2 exchange in natural waters. *Limnology and Oceanography 41*, 689–697, doi: 10.4319/lo.1996.41.4.0689.

Weiss R.F. 1974. Carbon dioxide in water and seawater: the solubility of a non-ideal gas. *Marine Chemistry 2*, 203–215, doi: 10.1016/0304-4203(74)90015-2.

Yamamoto S., Alcauskas J.B. & Crozier T.E. 1976. Solubility of methane in distilled water and seawater. *Journal of Chemical and Engineering Data 21*, 78–80, doi: 10.1021/je60068a029.

Zappa C.J., McGillis W.R., Raymond P.A., Edson J.B., Hintsa E.J., Zemmelink H.J., Dacey J.W.H. & Ho D.T. 2007. Environmental turbulent mixing controls on air–water gas exchange in marine and aquatic systems. *Geophysical Research Letters 34*, L10601, doi: 10.1029/2006GL028790.